WELDING RESEARCH

SUPPLEMENT TO THE WELDING JOURNAL, NOVEMBER 1976

Sponsored by the American Welding Society and the Welding Research Council

Material Variables Affecting Lamellar Tearing Susceptibility in Steels

Detailed investigation shows the tendency to lamellar tearing is too complex a phenomenon to fit the more commonly accepted susceptibility criteria

BY S. GANESH AND R. D. STOUT

ABSTRACT. A quantitative weldability test was employed to determine the lamellar tearing susceptibility of steels with a variety of melting and deoxidation practices, compositions and thicknesses. The degree was examined to which susceptibility was related to inclusion type and distribution, oxygen content, microstructural features, and fracture mechanisms. While tearing was generally associated with the elongated nonmetallic inclusions, in some steels initiation occurred by splitting along ferrite bands, liquation or intergranular cracking. Susceptibility was observed to increase with an increase in the oxygen content of the steel, but the inclusion count obtained using the Quantimet 360 did not show a satisfactory correlation. Voids formed either by decoherence or cracking of inclusions, and terrace linkage of adjacent voids occurred by several modes such as necking, microvoid coalescence, quasi-cleavage and intergranular cracking. Susceptibility was dependent on the nature of void formation, extent of void growth and the mode of void linkage. Techniques are listed for improving material resistance to lamellar tearing.

S. GANESH is with the Bendix Research Laboratories, Southfield, Michigan, and R. D. STOUT is Dean, Graduate School, Lehigh University, Bethlehem, Pennsylvania.

The work was sponsored by the Welding Research Council and was presented at the 57th AWS Annual Meeting held at St. Louis, Missouri, May 10-14, 1976.

Introduction

Lamellar tearing, a form of cracking occurring in planes essentially parallel to the rolled surface of a plate under high through-thickness loading, tends to initiate by the decoherence or cracking of elongated inclusions. Voids form which grow and link together by the plastic tearing of the intervening matrix, along the horizontal and the vertical planes, producing a characteristic step-like appearance to the fracture. Though welding is not a necessary condition, lamellar tearing has been generally associated with welded joints and occurs in the base metal with insufficient short-transverse ductility when subjected to high through-thickness strains generated if weld thermal contraction is inhibited by structural restraint.

Tearing typically occurs in the multipass weldments of T, corner, or cruciform joints and is reported in building construction (Refs. 1-4), bridge girders (Ref. 5), pressure-vessels (Ref. 6), shipbuilding (Ref. 7), off-shore structures (Ref. 8), boilers (Refs. 8, 10) and nuclear power plants (Ref. 11). Though, in most cases, the risk of tearing can be avoided through proper modifications to joint design and welding conditions (Refs. 12, 13), there are situations where the only choice is to select a costlier material having a high resistance to tearing.

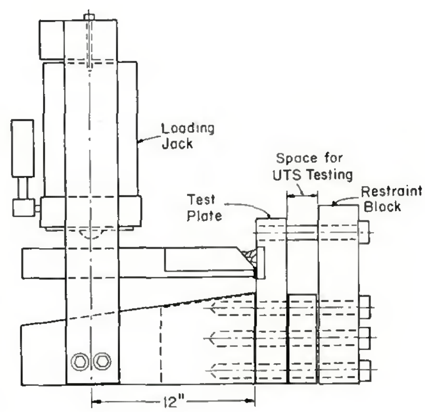

Fig. 1 — Lehigh lamellar tearing fixture

Thus, the problem of lamellar tearing has aroused much concern (Refs. 1-4, 14) among designers, steel manufacturers and fabricators; and research efforts have been aimed towards developing weldability tests to assess material susceptibility to

lamellar tearing and to correlate the susceptibility to short-transverse tensile and notch ductility, inclusion distribution, and ultrasonic measurements.

Despite numerous investigations, limited agreement has emerged on the factors responsible for tearing. There are conflicting opinions regarding the influence of factors such as melting and deoxidation practice (Refs. 7, 15, 16), plate thickness (Refs. 15, 17-19), rolling direction (Refs. 9, 20), inclusion type and distribution (Refs. 7, 10, 16, 21-26), strain aging (Refs. 22, 23, 27, 28), banding (Refs. 9, 29, 30), hydrogen (Refs. 21, 23, 28, 31), heat input, and preheat (Refs. 19, 22, 27, 31). Uncertainty also exists about the mechanism of tearing, its location (Refs. 20-22, 32) as well as the time and temperature of its occurrence (Refs. 17, 20, 23, 27).

According to some investigators (Refs. 20, 27) lamellar tearing is an elevated temperature phenomenon occurring in the temperature range 200-300 C while others (Refs. 17, 23) report it to be a form of delayed cracking occurring at room temperature a few hours after welding. The tears are reported to initiate at the toe or root of the weld or anywhere within the base metal from the fusion zone to the center of plate thickness.

Attempts to correlate lamellar tearing susceptibility to through-thickness tensile and notch ductility, inclusion distribution, or ultrasonic measurements have not been very successful, partly due to a lack of quantitative data on the tearing susceptibility and partly due to complexity of the phenomenon itself.

In an attempt to alleviate this situation a weldability test was developed at Lehigh (Ref. 22) to provide a quantitative measure of susceptibility to lamellar tearing (Fig. 1), The test consisted of joining a cantilever to a rigid vertical test plate by depositing a multipass weld in a 45 deg bevel groove while maintaining constant levels of through-thickness stress by externally loading the cantilever. The stress level just necessary to cause failure during testing, without the need for an overload, designated the critical weld restraint level (CWRL), was chosen as the criterion to represent the lamellar tearing susceptibility.

In the present investigation, the material variables controlling the cracking phenomenon were studied by the Lehigh test to determine the susceptibilities of a range of steels and to examine the roles of material parameters and fracture mechanisms in tearing.

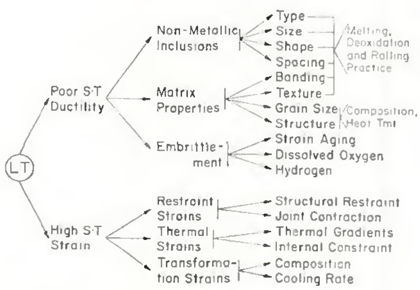

Fig. 2 — Variables in lamellar tearing

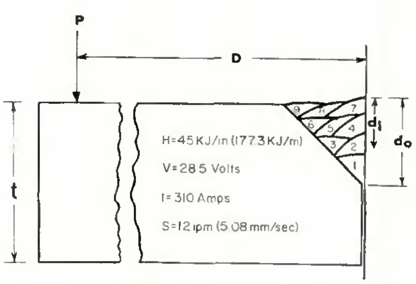

$$P = \frac{(WRL)\ w\ (do-di)\quad (t-do)+\frac{do-di}{2}}{D}$$

W = width of the test plate

di = distance from the top of the i th weld layer to the top of the cantilever plate

Fig. 3 — Welding sequence

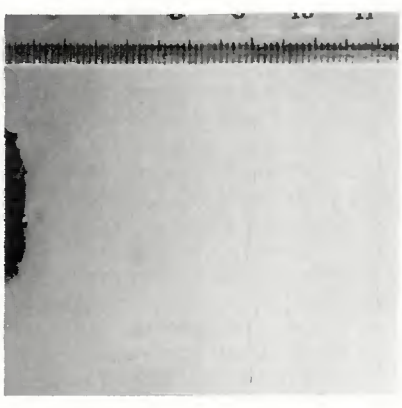

Fig. 4 — Failure close to the plate surface despite the opening up of centerline laminations in Si killed A515-65 (Y) steel

Variables in Lamellar Tearing

In a welded joint, lamellar tearing may be expected to initiate when and wherever the through-thickness strain exceeds the ductility. While the overall weldment strain depends on the degree of joint contraction and the restraint intensity of the surrounding structure, the local stress-strain distributions are highly heterogeneous and result from the complex interaction of weld thermal gradients and the constraint imposed by the surrounding continuum. The through-thickness ductility is governed by metallurgical variables such as type, size, shape and spacing of nonmetallic inclusions, laminations, properties of the intervening matrix, crystallographic texture, banding, and embrittling mechanisms that may act during (or after) welding to lower the local ductility. These, in turn, are influenced by a variety of factors such as melting, deoxidation and rolling practice, material composition, heat treatment, presence of hydrogen, dissolved oxygen, strain aging, structural restraint, welding conditions, etc. The variables controlling the tearing phenomenon are schematically illustrated in Fig. 2 and, among them, the elongated nonmetallic inclusions are probably the prime cause of poor through-thickness ductility.

Nonmetallic Inclusions

The reported (Refs. 10, 15, 22, 26) lack of a direct correlation between the inclusion content and lamellar tearing susceptibility suggests that efforts to achieve steel cleanness are not necessarily the most economical methods of achieving improvement in lamellar tearing resistance. The cost and cleanness of steel are influenced by the route followed during steel making and the best route is one which would provide, at a minimum cost, the least harmful inclusions as regards their type, size, shape, and distribution.

The shape and size of inclusions after forming operations depend on their formability characteristic which is influenced by their composition and the working condition. Silicates are not deformable at room temperature but deform at higher temperature, the extent of which depends on their composition (Refs. 33, 34). Spinels, alumina and calcium aluminates do not deform at temperatures encountered in steel rolling and retain their globular shape whereas the monophase type III MnS are highly deformable and elongate to form stringers (Refs. 33, 34).

Depending on the degree of deoxidation, sulfide inclusions may be either type I, II, or III. While type III sulfides are formed in steels thoroughly deoxidized with an excess of aluminum, the type I oxysulfides occur in rimmed, semikilled or silicon killed steels where the oxygen content of the liquid steel is relatively high (Refs. 35-37). The type II sulfides occur as a dendritic network in steels having an intermediate oxygen content and form closely connected groups of elongated inclusions after rolling. Increasing additions of zirconium and rare earth metals lead to a modification of the sulfide morphology, the inclusions formed tending toward equiaxed angular particles or spheres (Ref. 35). Unlike type III, these

'alloyed' sulfides resist deformation and retain their globular shape. Injection of silicon-calcium, aluminum-calcium or misch metal under a highly basic slag is reported (Ref. 38) to reduce sulfur contents to below 0.005 percent.

In Si killed steels, the major inclusions are the multiphase silicates, while the minor ones are type I sulfides and simple oxides. With simultaneous Si-Al deoxidation the inclusions formed display a wide range of composition and morphology due to complexity of the reactions and are of the type $M_xA_YS_Z$ (manganese aluminum silicates), $A_Y S_Z$ (mullite) and a mixture of type I and III sulfides (Ref. 39). If Al deoxidation is carried out before Si addition, the major inclusions are the monophase type III sulfides and the minor ones are alumina, spinels and calcium aluminates. One can, thus, anticipate lamellar tearing to initiate at the silicates in Si killed and semikilled steel and at the sulfides in an Al killed steel.

The propensity for void formation depends on the differential thermal expansion characteristics between the inclusion and steel matrix. Where the inclusions contract more than the matrix, as with sulfides and iron oxides, voids tend to form; but if the inclusions contract less than the matrix, as with silicates, tessellated stresses are generated (Refs. 40, 41).

Among the techniques available for inclusion counting, the Quantimet is reported (Refs. 42, 43) to give accurate and reproducible measurements. Nevertheless, at the magnifications normally employed for the assessment of steel cleanness, it is not possible to account for the smaller inclusions — especially the oxides — which may exert significant influence on the lamellar tearing susceptibility. In some steels, especially the Al killed type, longitudinal streak-like defects containing aligned clusters of small alumina inclusions occur which apparently result from reoxidation during teeming and get entrapped in the ingot during solidification. Such defects may not be included in the Quantimet data and the steel quality may be overestimated.

Beside the effects of inclusions and laminations, other factors like banding, crystallographic texture and matrix embrittlement may play a significant role in enhancing the mechanical anisotropy of rolled products. While the significance of banding with regard to lamellar tearing is not established yet, the through-thickness ductility is reported (Refs. 29, 45) to drop with an increase in the degree of banding. A homogenizing treatment has been reported (Refs. 15, 16, 26, 29, 45) to eliminate the effects of banding, but Jatczak et al (Ref. 46) and Grange (Ref. 47) concluded that homogenization causes only slight, commercially insignificant improvements in the transverse ductility and impact strength.

Some steels, especially the controlled rolled type, have been reported (Refs. 48-50) to exhibit periodic splitting parallel to the rolling plane and this has been attributed to cleavage along textured ferrite bands (Ref. 48), tearing along deformed ferrite grain boundaries containing numerous carbides (Ref. 49) and separation along embrittled sulfide interfaces (Ref. 50). Splitting is reported (Ref. 48) even among the rare earth treated steels containing low sulfur levels with shape control. Also, the habit planes of martensite laths, formed from unrecrystallized austenite, tend to have preferred orientation due to the texture in the parent austenite and this may contribute to splitting in the matrix.

The matrix ligament separating the inclusion voids may be embrittled, either during or after welding, by factors such as strain aging, dissolved oxygen, hydrogen, etc., thus facilitating lamellar tear initiation. Jubb et al (Ref. 27) have shown that in multipass welds, the HAZ of the parent material passes through a temperature range where limited ductility combined with a tendency to strain aging is likely to be experienced. The maximum strain aging is found to develop at temperatures in the range of 250-300 C. The strain aging may rapidly embrittle the matrix ligaments separating the inclusion voids so that these ligaments fracture at low strains. As little as 20-30 ppm of oxygen in solution is reported (Ref. 51) to produce a marked intergranular embrittlement of iron without a significant rise in the yield stress and increasing quantities of oxygen are found to be progressively embrittling.

There is limited evidence (Refs. 21, 23, 28) to suggest that lamellar tear-

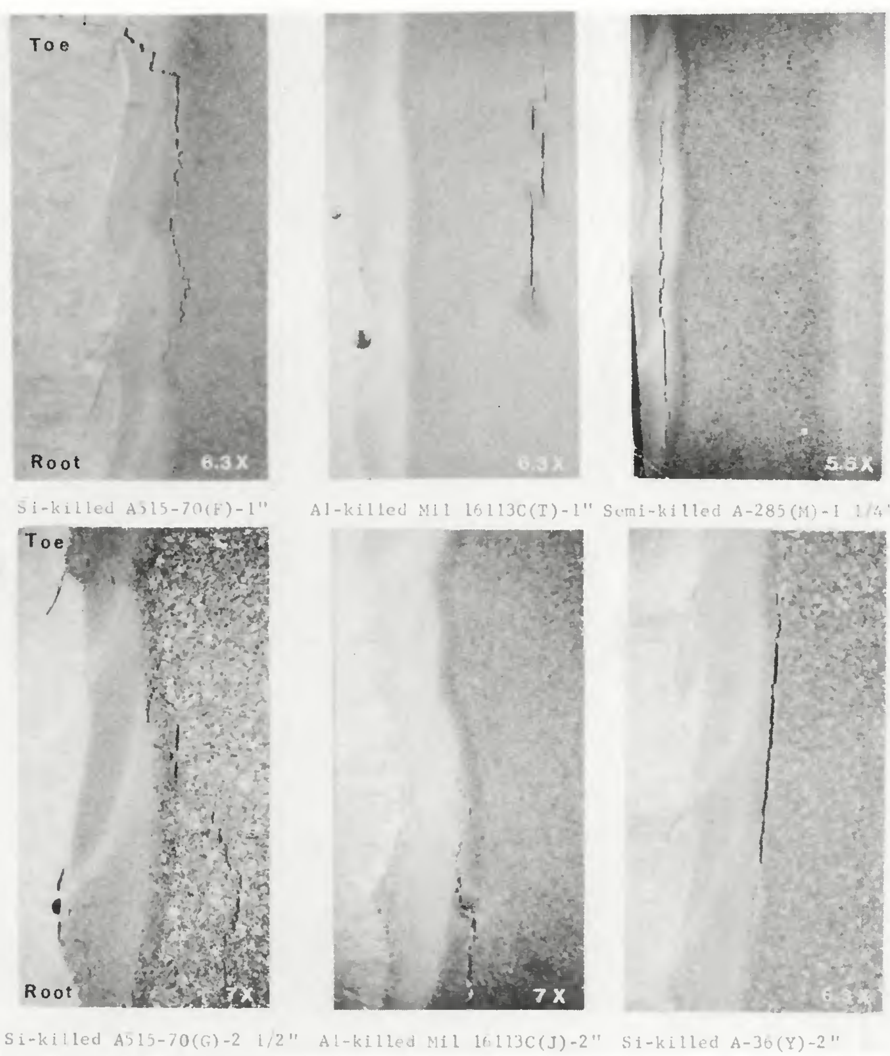

Fig. 5 — Location of lamellar tears in various steels. (Reduced 33%)

Table 1 — Material Details

No.	Material	Thickness, in.	Code	History of lamellar tearing[(a)]	C	Mn	P	S	Si	Ni	Cr	Cu	Al	Sn	N	O	Others
										Composition							
				Semikilled Steels													
1	A285-C	1¼	M	Fab. failure	.22	.41	.002	.027	.06	.12	.06	.25	<.005	.007	.0050	.009	—
2	A36	1½	X	Reported	.23	.78	.011	.027	.06	.01	.02	.01	<.005	<.002	.005	.0100	0.01 Ce
				Silicon Killed Steels													
3	F. M. grade	3¾	N	Unknown	.24	1.24	.005	.17	.32	.15	.07	.18	<.005	<.005	.0060	.0035	0.2 Pb
4	A515-70 (b)	2½	G	Fab. failure	.30	.83	.005	.029	.23	.07	.03	.075	<.005	.005	.0070	.014	—
5	A515-70	1	F	Reported	.25	.73	.005	.024	.28	.02	.02	.052	<.005	<.002	.0047	.0042	0.006 Ce
6	A515-65	3¼	V	Reported	.23	.56	.008	.031	.26	.13	.15	.24	<.005	.017	.0054	.0026	0.06 Mo, 0.011 Ce
7	A515-71	2½	K	Reported	.29	.70	.002	.021	.22	.16	.07	.32	<.005	.018	.0082	.0022	—
8	A36	2	Y	Reported	.27	1.04	.011	.015	.25	.01	.04	.014	<.005	<.002	.0059	.0087	0.006 Ge
9	EH-33	¾	P	Fab. failure	.14	1.37	.018	.019	.37	.02	<.01	.03	.002	<.005	.0072	.0071	0.015 V, 0.008 Ti, 0.006 Ce, 0.03 Nb
10	A283 Gr.D	8	C	Fab. failure	.20	.54	.004	.019	.26	.14	.09	.21	.005	.012	.0078	.0081	—
11	A283	5	B	Fab. failure	.29	.54	.011	.021	.17	<.01	<.01	.006	.010	<.002	.0041	.0033	—
				Aluminum Killed Steels													
12	A516-70	1	E	Reported	.24	1.22	.009	.021	.26	.11	.06	.15	.058	.004	.0072	.0038	—
13	A516-71	2¾	R	Unknown	.26	1.09	.008	.023	.26	.11	.10	.15	.044	.007	.0050	.0021	—
14	Mil 24113C	1	U	Reported	.15	1.24	.011	.019	.29	.20	.17	.086	.047	.002	.0064	.0069	—
15	Mil 16113C	1	T	Reported	.15	1.34	.010	.030	.30	.03	.03	.26	.062	.04	.0061	.0026	0.048 V, 0.035 Ti
16	A588 Gr.D	1	W	Fab. failure	.14	1.23	.010	.022	.28	.30	.58	.34	.089	.006	.0079	.0021	0.027 V, 0.06 Ti, 0.011 Ce
17	A533 Gr.B	5⅞	D	Unknown	.25	1.38	.010	.012	.24	.54	.21	.13	.038	.007	.0060	.0032	0.6 Mo
				Rare Earth Metal Treated													
18	Z-Steel	1½	S	Unknown	.065	1.38	.012	.002	.65	.08	.10	.06	.075	.008	.011	.0017	0.025 Ce, 0.1 Nb

(a) Fab. Failure — The material was cut out from the plate which had exhibited lamellar tearing during fabrication.
Reported — Lamellar tearing is reported in this grade, but the material tested came from a different heat.
Unknown — No case history of lamellar tearing exists for this material.

(b) Tested by Oates and Stout (Ref. 23).

ing is a form of delayed cracking occurring at room temperature a few hours after welding. Several investigators (Refs. 52-55) have reported on the beneficial effect of sulfides which, acting as hydrogen sinks, tend to lower the hydrogen activity in the lattice and, thus, reduce the likelihood of underbead cracking. However, if voids and microcracks are formed around inclusions, as is the case in lamellar tearing, the presence of occluded hydrogen may increase the likelihood of subsequent propagation by hydrogen assisted cracking (Refs. 55, 56).

Materials and Procedure

A range of materials which included two semikilled, eight silicon killed, six aluminum killed, one rare earth treated and one leaded-sulfurized steel, with the thickness ranging from 18 mm to 400 mm (3/4 in. to 8 in.) were tested to evaluate their tearing susceptibility. These steels were supplied by various manufacturers and fabricators — some coming from portions of a structure that had displayed lamellar tearing during actual fabrication, some belonging to grades that have had reported histories of lamellar tearing and some that have had no known history of lamellar tearing. The material details are presented in Table 1.

The lamellar tearing susceptibilities of the various steels were determined with the Lehigh test procedure outlined by Oates and Stout (Ref. 22). This test was developed to provide a simple and effective means of evaluating the lamellar tearing susceptibility of various materials through the application of an external load to supplement the weld thermal and restraint stresses. The external load was increased proportionally to the cross sectional area of the weld after each weld layer had cooled to room temperature so as to maintain a given level of through-thickness stress, called the weld restraint level, which was characteristic of each test. The load required was calculated using the simple formula given in Fig. 3 and the restraint level just enough to cause failure during welding, called the CWRL, was used as the susceptibility criterion.

In determining this criterion, care was taken to see that plates less than 38 mm thick were stiffened by welding a 25 mm thick back-up plate to them so that the longitudinal stresses due to bending between the restraining bolts was small compared to the through-thickness stresses. Thus, the CWRL could be related to the material parameters without having to consider the variable effects introduced through changes in the plate stiffness (thickness).

An automatic gas metal-arc (GMA) welding process was used and the welding conditions employed are listed in Table 2. The extent and nature of subcritical tears were studied by metallographic examination of sections taken from the specimens tested just below the CWRL and microhardness measurements were carried out at regions around the tears to gain additional understanding of the factors influencing tear location.

The inclusion distributions in the various steels were evaluated using the Quantimet 360. Areas approximately 5 mm below the plate surface were scanned as the tears have been observed to lie mostly in this zone. Fifty fields were scanned in each section and a minimum of four sections were examined for each material so as to give adequate sampling. The average values of area fraction (A), aspect ratio (λ), number of inclusions (N), inclusion length (L) and the longest inclusion in each field (L_x) were determined. The inclusions were identified both from the polished sections, using the electron microprobe, as well as from the fracture surface, using the energy dispersive spectrometer (EDS) associated with the SEM. The oxygen contents of the steels were determined by the vacuum fusion method and represent both dissolved and combined oxygen. Fractographic studies were carried out on the SEM by examining various regions on the fracture surface and stereopictures were taken to assist in better interpretation of the fracture features.

Results

Behavior of the Various Steels

The Lehigh lamellar tearing test results are presented in Table 3 and the susceptibility of the various steels are summarized in Table 4 together with information on their composition, matrix structure, inclusion type and distribution, tear location, fracture mode, etc. From Table 4 it can be seen that different heats of steel of the same grade display a wide variation in tearing susceptibility.

For instance, the susceptibility (CWRL) of Si killed A515-70 grade varied from 44 ksi (303 MPa) for the G-heat to 61 ksi (421 MPa) for the F-heat to 71 ksi (490 MPa) for the K-heat. The 80 mm (3.15 in.) thick A515-65 (V) plate showed a high resistance to tearing despite a heavy centerline lamination and, though the

Fig. 6 — Crack initiation by mechanisms other than lamellar tear. (Reduced 54%)

Table 2 — Welding Conditions

1. Filler metal[a]	Aircomatic A-632, 0.045 in. (1.143 mm) UTS = 123 ksi (848 MPa) YS = 109 ksi (752 MPa) % Elong = 22 RA = 65 CVN at −50 C = 70 ft-lb (95 J)
2. Shielding gas	Argon + $2/O_2$
3. Gas flow rate	50 cfh (23.6 l/min)
4. Current	315 A
5. Voltage	28 V
6. Travel speed	12 ipm (5 mm/s)
7. Electrode extension	¾ in. (19 mm)
8. Inter-pass temperature	Room temperature
9. Number of passes	Nine (9)
10. Heat input	45 kJ/in. (178 kJ/m)

(a) Composition: .07 C, 1.35 Mn, .50 Si, .012 S, .01 P, .45 Mo, 1.30 Ni, .15 V

Table 3 — Results of Lamellar Tearing Tests

Material	Specimen	WRL ksi	WRL (MPa)	Failure	Fracture stress ksi	Fracture stress (MPa)	Remarks	CWRL ksi	CWRL (MPa)
F.M. Grade (N)	7NA1	55	(379)	Yes	—	—	Failed, loading after 3rd pass		
1⅞ in. from	7NA2	40	(276)	Yes	—	—	Failed, loading after 6th pass		
3¾ in. plate	7NA3	28	(193)	No	37.5	(259)	—	37	(255)
	7NA4	36	(248)	No	37	(255)	—		
	7NA5	35	(241)	No	—	—	Metallographically examined		
EH 33 (P)	7PA1	50	(345)	Yes	—	—	Failed, loading after 6th pass		
¾ in.	7PA2	44	(303)	No	46	(317)	—		
	7PA3	46	(317)	Yes	45	(310)	Failed, loading after 9th pass		
	7PA4	42	(290)	No	—	—	Metallographically examined		
A516-70[a] (E)	7EA1	55	(379)	Yes	—	—	Failed, loading after 8th pass		
1 in.	7EA2	50	(345)	Yes	—	—	Failed, loading after 9th pass	50[a]	(345)
	7EA3	45	(310)	No	51	(352)	—		
	7EA4	45	(310)	No	—	—	Metallographically examined		
A285-C (M)	7MA1	52	(359)	No	53	(365)	—		
1¼ in.	7MA2	60	(414)	Yes	—	—	Failure after 6th pass	53	(365)
	7MA3	56	(386)	Yes	—	—	Failure after 6th pass		
	7MA4	48	(331)	No	—	—	Metallographically examined		
Mil-24113C (U)	7UA1	64	(441)	Yes	—	—	Failed, 10 h after loading		
1 in.	7UA2	60	(414)	Yes	—	—	Failed, loading after 6th pass	58	(400)
	7UA3	57	(393)	No	58	(400)	—		
	7UA4	56	(386)	No	—	—	Metallographically examined		
A515-70 (F)	7FA1	65	(448)	Yes	—	—	Failed, loading after 7th pass		
1 in.	7FA2	50	(345)	No	62	(428)	—	61	(421)
	7FA3	60	(414)	No	61	(421)	—		
	7FA4	58	(400)	No	53	(365)	Metallographically examined		
A516-70 (R)	7RA1	60	(414)	No	64	(441)	—		
2¾ in.	7RA2	72	(496)	Yes	—	—	Failed after 2nd pass	62	(428)
	7RA3	64	(441)	Yes	—	—	Failed after 4th pass		
	7RA4	62	(428)	Yes	—	—	Failed, 10 h after loading		
	7RA5	58	(400)	No	—	—	Metallographically examined		
Mil-16113C (T)	7TA1	56	(386)	No	67	(462)	—		
1 in.	7TA2	62	(428)	No	67	(462)	—		
	7TA3	68	(469)	Yes	—	—	Failed, loading after 9th pass at 64 ksi	66	(455)
	7TA4	64	(441)	No	—	—	Metallographically examined		
A-36 (Y)	7YA1	60	(414)	No	67	(462)	—		
2 in.	7YA2	68	(469)	Yes	—	—	Failed after 4th pass		
	7YA3	64	(441)	No	67	(462)	—	67	(462)
	7YA4	66	(455)	No	—	—	Metallographically examined		
A-36 (X)	7XA1	56	(386)	No	68	(469)	—		
1½ in.	7XA2	68	(469)	No	69	(476)	—		
	7XA3	72	(496)	Yes	—	—	Failed, loading after 8th pass	69	(476)
	7XA4	68	(469)	No	—	—	Metallographically examined		
A515-65 (V)	7VA1	64	(441)	No	70	(483)	—		
3¼ in.	7VA2	70	(483)	Yes	—	—	Failed, loading after 9th pass		
laminated	7VA3	67	(462)	No	—	—	Laminations opened at center	69	(476)
A533 Gr.B (D)	7DA1	56	(386)	No	—	—	Failed in weld after 7th pass		
2 in. from 5⅞ in. pl.	7DA2	52	(359)	No	no failure at 74	(495)	Metallographically examined		
	7DA3	76	(524)	Yes	—	—	Failed along HAZ after 3rd pass	70	(483)
	7DA4	72	(496)	Yes	—	—	Failed along HAZ after 5th pass		
	7DA5	65	(448)	No	70	(483)	—		
A515-70 (K)	7KA1	52	(359)	No	72	(496)	—		
2½ in.	7KA2	72	(496)	Yes	—	—	Failed after 24 h at 72 ksi		
	7KA3	68	(469)	No	71	(490)	Failure after 6th pass	71	(490)
A588 Gr.A (W)	7WA1	56	(386)	No	77	(531)	—		
1 in.	7WA2	76	(524)	Yes	—	—	Failed while restoring load to 76 ksi, 15 h after welding	75	(517)
	7WA3	72	(496)	No	75	(517)	Failed while overloading 18 h after welding		
Z Steel (S) 1½ in.	7SA1	60	(414)	No	77	(531)	Failed in the weld metal	>75	(517)
A283 Gr.D 3 in. from	7BA1	52	(359)	No	83	(572)	Failed near HAZ		
8 in. plate	7BA2	72	(496)	No	>75	(517)	Metallographically examined	>75	(517)
A283 2⅝ in. from 5 in. plate	7CA1	60	(414)	No	>75	(517)	No failure but ultrasonic indications after overloading	>75	(517)

(a) Tested without stiffener

Fig. 7 — Array of parallel cracks in semikilled A-285 (M) steel

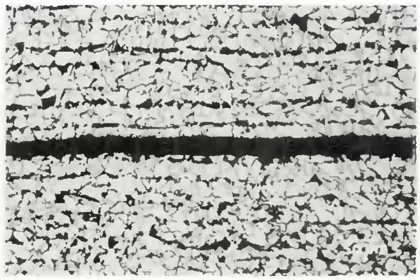

Fig. 8 — Terrace crack through a ferrite band in Al killed Mil 24113C (U) steel

Fig. 9 — Fracture surface showing lamellar tear initiation (right) and cleavage propagation (left) in semikilled A-285 (M)

laminations opened up under load (Fig. 4), failure occurred close to the plate surface, suggesting that tearing susceptibility is mostly influenced by the material condition close to the plate surface.

Among the materials that had exhibited lamellar tearing during actual fabrication, the ABS EH-33 (P), A-285 (M) and A515-70 (G) displayed a high susceptibility (low CWRL) in the Lehigh test whereas the A-283 (heat B and C) steels showed a low susceptibility (high CWRL). This showed that a material with inherently high resistance to tearing may suffer lamellar tearing, but only if the restraint conditions are severe enough. The rare earth-treated Z-steel exhibited a high resistance to tearing and failed in the weld metal rather than the base metal, thereby demonstrating the beneficial effects of rare earth additions on the tearing susceptibility. There was no definite trend in the susceptibility with variations in the plate thickness.

Nature and Location of Tears

In the Lehigh test, the tearing tended to initiate while the arc was midway through the pass, in the end portion of the plate, adjacent to the toe of the preceding layer. This was due, apparently, to a transient overload occurring at the end portion of the weld from a reduction in the net section supporting the external load as the molten puddle entered the junction of start tab and test plate. Metallographic examination of subcritical tears showed lamellar tears to initiate anywhere from the lower part of the HAZ to locations up to 13 mm below the plate surface (Fig. 5).

However, in EH-33 and the free machining steel the crack initiated close to the fusion zone, apparently by liquation, and propagated as a lamellar tear (Fig. 6). In A533 Gr. B steel, tearing occurred in the coarse grained HAZ by a combination of intergranular cracking and lamellar tearing (Fig. 6).

For the same plate thickness, the depth location of tearing tended to be maximum in the Al killed steels (Mil 24113C, Mil 16113C), intermediate for the Si killed steel (A515-70) and minimum in the semikilled steel (A285) (Fig. 5). In the semikilled and Si killed steels, extensive tearing was observed outside the main crack front (Fig. 7) but not so in the Al killed steels. In banded steels there was a tendency for the terrace crack to run within the ferrite bands (Fig. 8).

The fracture surface (Fig. 9), often displayed a region of ductile lamellar tear initiation and a region of brittle cleavage propagation, the proportion of which varied depending on the material parameters and the test condition. In Al killed A516-70, Mil 24113C and Mil 16113C steels, 100% ductile fracture was observed (Fig. 10), while other steels displayed varying proportions of lamellar tear and cleavage.

On a microscopic scale, lamellar tears were characterized by a step-like pattern with stacks of terraces linked together by shear walls (Fig. 11). The terrace cracks displayed an array of elongated voids whose size and density varied among the different steels depending on their susceptibility (Fig. 12). The voids tended to be larger and denser in the more susceptible steels. Though the terrace was generally associated with the inclusion voids, in some steels they showed the following features (Fig. 13): (a) splitting along laminations, (b) network of a liquated phase along prior austenite grain boundaries (only in EH-33 and F.M. Steel), and (c) clusters of equiaxed dimples containing oxides (MnO, alumina, etc.) and sulfides (MnFeS, Type I MnS).

In EH-33 (P) steel, the terrace displayed a dense network of a liquated phase which was enriched in Si, Al, Mn, Fe, S, Nb, Ca and Ti (Fig. 14) and in the leaded-sulfurized steel (N), the terrace was characterized by both elongated sulfide inclusions and a dense network of FeS containing clusters of small (MnFe)S inclusions (Fig. 15).

Fig. 10 — Fracture surface showing 100% ductile lamellar tear in Mil 24113C (U)

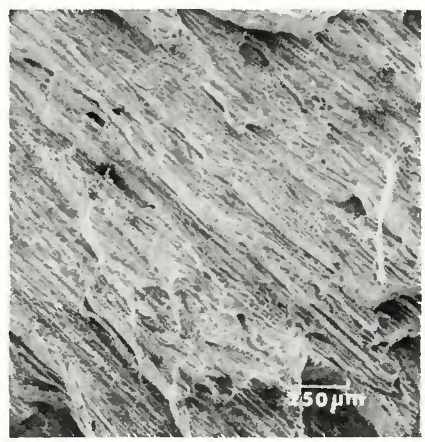

Fig. 11 — Stacks of terraces linked together by shear walls in Si killed A515-70 (F)

Inclusion Characteristics

Typical inclusions within voids on the fracture surface of some steels are shown in Figs. 16, 17 and 18, and inclusion distribution in various steels are shown in Fig. 19. While the inclusion types present were chiefly influenced by the deoxidation practice, their composition varied with the relative proportion of deoxidizing elements present.

For instance, in the semikilled A-285, which had a low Mn content (0.41), the oxides and silicates were found to be highly enriched in Fe, whereas in the semikilled A-36, containing nearly twice the Mn (0.78) and some Ce (0.01), the proportion of Fe in the oxides was much less. Silicate

Table 4 — Summary of Observations on Various Steels

Material and thickness	Matrix structure[a]	Inclusion type major	Inclusion type minor	%A	Inclusion count L X10^{-2}	λ	N	L_x	CWRL ksi	Location of tears	Fracture mode initiation	Fracture mode propagation
F.M. Steel (N) 3¾"	Elongated F + P G = 3	Type II Sulfides	Type II MnS PbS, (Fe, Mn) O	1.00	15.58	1.7	7.0	64	37	Upper HAZ	Liquation	L•T
EH-33 (P) ¾"	Very fine grained Banded F + P, G = 9	Silicates	Type III MnS	.17	23.97	2.7	8.0	61	45	Upper HAZ	Liquation + Splitting	L•T
A-285 (M) 1¼"	Randomly oriented F + P, G = 3	Silicates	Type III MnS FeO, MnO	.23	26.3	3.1	10.3	64	51	Lower HAZ	L•T	Cleavage
A-36 (X) 1½"	Elongated F + P G = 3	Silicates	Type III MnS, MnO	.35	28.1	3.4	15.0	114	67	Lower HAZ	L•T	Cleavage
A515-70 (G) 2½"	Elongated F + P G = 3			.37	22.4	1.9	14.0	82	44	Below HAZ	L•T	Cleavage
A515-70 (F) 1"	Elongated F + P G = 3			.09	13.7	1.5	6.4	29	61	Below HAZ	L•T	Cleavage
A515-65 (V) 3¼"	Randomly oriented F + P, G = 3	Silicates	Type III MnS (Mn, Fe) O	—	—	—	—	—	69	Lower HAZ	L•T	Cleavage
A515-71 (K) 2½"	Randomly oriented F + P, G = 3			.08	9.89	1.0	8.2	16	71	—	MVC	Cleavage
A-36 (Y) 2"	Ferrite needles + P, G = 2			.29	24.9	3.0	14.0	80	69	Below HAZ	L•T	Cleavage
Mil 24113C (U) 1"	Severe banding G = 7			.10	18.8	2.1	5.9	40	58	~ 3/16 in. below HAZ	L•T	L•T
A516-71 (R) 2¾"	Severe banding G = 6	Type III MnS	Alumina	.12	18.1	2.2	8.1	38	62	Below HAZ	L•T	Cleavage
Mil 6113C (T) 1"	Moderate banding G = 8			.15	17.2	1.9	9.6	55	66	~ 1/4 in. below HAZ	L•T	L•T
A533 Gr.B (D) 5⅞"	Tempered bainite G = 9	—	Type III MnS	.07	14.1	1.9	6.7	21	70	Upper HAZ	MVC	MVC
A588 (W) 1"	Equiaxed F + P G = 5	Type III	Alumina	.07	12.2	1.6	7.6	22	75	Lower HAZ	L•T	Cleavage
Z-Steel (S) 1½"	Equiaxed F + P G = 8	—	R. E. oxides	.11	7.54	1.1	21	14	>75	Weld	MVC	MVC

(a) F = Ferrite, P = Pearlite, G = ASTM Grain Size Number

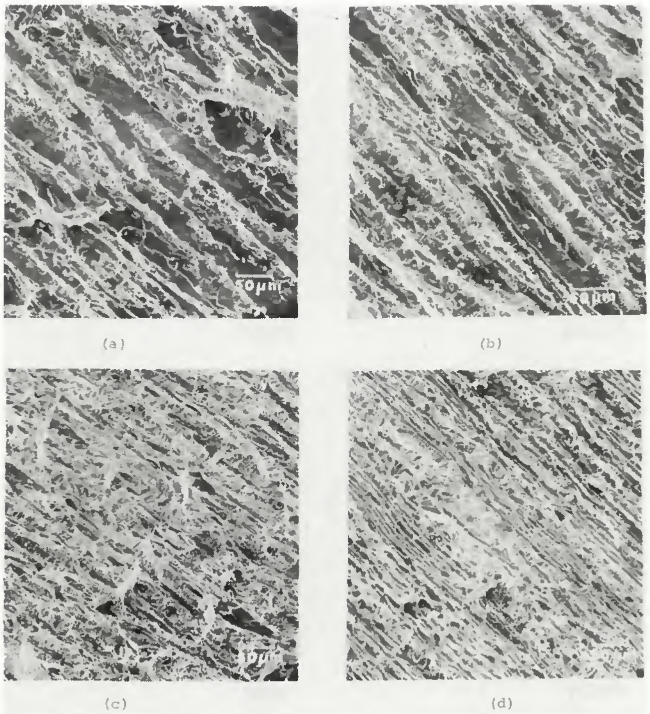

Fig. 12 — Array of inclusion voids on the terrace of various steels. (a) Mil 24113C (U); (b) A516-70 (E); (c) Mil 16113C (T); (d) A588 (W). (X200, reduced 52%)

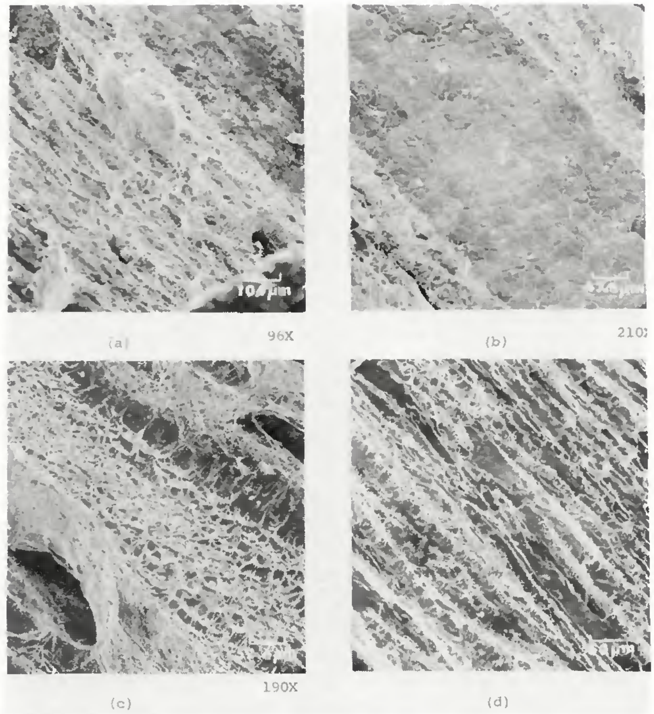

Fig. 13 — Types of terrace cracks: (a) splitting along laminations; (b) network of a liquated phase; (c) cluster of equiaxed dimples containing alumina; (d) array of elongated voids. (Reduced 52%)

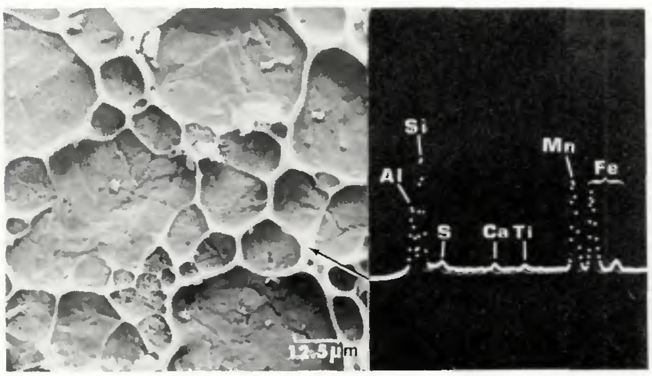

Fig. 14 — Liquated phase in EH-33 (P) steel

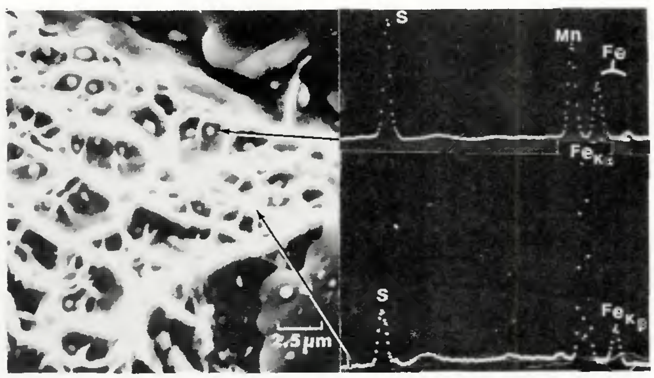

Fig. 15 — Liquated FeS network containing (Mn, Fe) S inclusions, in Pb-sulfurized F. M. steel (N). (Reduced 41%)

inclusions were mostly in the form of stringers (Fig. 19a) whereas the sulfides were present in a wide range of shapes and sizes. Type I MnS was often duplex with a eutectic tail surrounding the monophase MnS and Type III MnS was generally present as a fine stringer (Fig. 19b). Clusters of small aluminate inclusions with polyhedral contours were found in the Al killed steels and, in some cases, they appeared as a continuous trail containing hundreds of inclusions (Fig. 19d).

The inclusion count obtained with the Quantimet did not show a satisfactory correlation with the lamellar tearing susceptibility, as indicated by the CWRL. Though susceptibility tended to be low among steels with a very low inclusion count — A515-70 (K), A588 (W), A533 Gr. B (D), Z steel (S) — some steels such as, A36-(X), A36-(Y) and Mil 16113C (T), displayed a low susceptibility despite their high inclusion count (Table 4).

Results from oxygen analysis showed lamellar tearing tendency to increase with an increase in the oxygen content of the steel (Fig. 20). However, the semikilled and Si killed A-36 steels displayed a high resistance to tearing despite their high oxygen content.

Mechanism of Tearing

The progressive stages in lamellar tearing are shown in Fig. 21 for the Si killed A515-70 material. The first stage was void formation which occurred either by decoherence of the inclusion-matrix interface or by cracking of inclusions. The second stage was the linking of adjacent voids on the same plane by the rupture of intervening matrix to form a terrace crack. And the final stage was the linking of terrace tears on adjacent planes by vertical shearing which gave the characteristic step-like appearance to the fracture.

While the smaller inclusions tended to separate by interface decoherence (Fig. 22) those with large aspect ratio often displayed multiple internal fracturing (Fig. 23). Silicates invariably shattered within the voids whereas the sulfides tended to decohere, unless the aspect ratio was very high (Fig. 24). Larger inclusions tended to form voids earlier than the smaller ones (Fig. 25). The

extent of void growth around inclusions varied among the different steels and tended to be greater in materials exhibiting a high resistance to tearing (Fig. 26).

When the inclusions were closely spaced, the voids tended to coalesce by necking (Figs. 27a, 28a) whereas when the inclusions were farther apart, the voids generally linked together by a sheet of microvoids containing small oxides and sulfides (Figs. 27b, 28b). The proportion of microvoids varied among the different steels and tended to be higher among the more susceptible steels. For instance, among the semikilled steels, A-285, which was more susceptible than A-36, contained a far greater proportion of microvoids on the terrace than the A-36 (Fig. 26). Similarly, among the Al killed steels, the proportion of alumina clusters was found to be considerably higher in Mil 24113C (U) than in Mil 16113C (T) (Fig. 13c). The latter steel displayed a greater resistance to tearing despite its higher inclusion count (i.e., type III MnS).

In a few rare instances, void linkage occurred in a "zig-zag" manner with ridges and valleys (Fig. 22c) and, in one material (A-533 Gr. B), the voids were joined by intergranular separation (Fig. 27d). Void linkage also occurred by quasi-cleavage and cleavage (Fig. 28d). In materials exhibiting cleavage propagation, islands of inclusion voids were often seen surrounded by cleavage facets, suggesting that voids had formed earlier in the fracture process while the ligaments connecting them cleaved during the final unstable propagation (Fig. 29). The vertical shear linkage of terrace cracks occurred late in the tearing process and was associated with microvoids (Fig. 30).

Discussion

Investigation of lamellar tearing susceptibility on a wide range of materials has shown that susceptibility to tearing is a function of many variables and cannot be generalized on the basis of steel grade, plate thickness, deoxidation practice, etc. This was evident from the wide variation in the susceptibility observed among different heats of steel of the same grade and also from the lack of correlation between susceptibility and plate thickness, inclusion type, or inclusion count.

This behavior was understandable from the fact that lamellar tearing is a complex phenomenon governed by a variety of mechanical and metallurgical factors.

Metallographic examination of subcritical tears in the various steels clearly showed lamellar tearing to occur in three distinct stages, namely: (a) void initiation, (b) void growth and (c) void linkage.

Void Initiation

This was observed to occur either by the decoherence of inclusion-matrix interface or by the cracking of inclusions. The latter effect was confined to large silicates or sulfides (Figs. 23 and 24). This may be because, as indicated by other investigators, (Refs. 57-61) larger inclusions tend to contain more flaws and, hence, are susceptible to internal fracture while the smaller inclusions, remain intact and nucleate voids by interface decoherence (Fig. 22). Argon et al (Ref. 62) have shown that for decoherence to occur, the local stress must exceed the interfacial strength. The magnitude of the interfacial stress is reported (Ref. 62) to be influenced by factors such as residual tessellated stress, inclusion aspect ratio, matrix flow strength and inclusion interactions, while the interfacial strength is dependent on the type of inclusion and the presence of impurities such as Sn, P, Sb, As, etc. which tend to embrittle the interface (Ref. 63).

The larger inclusions were observed to form voids earlier than the smaller ones as was evident from the presence of undamaged smaller inclusions lying beside a fractured or decohered larger inclusion (Figs. 23, 24). This fact implies that, at a given volume fraction of inclusions, uniform

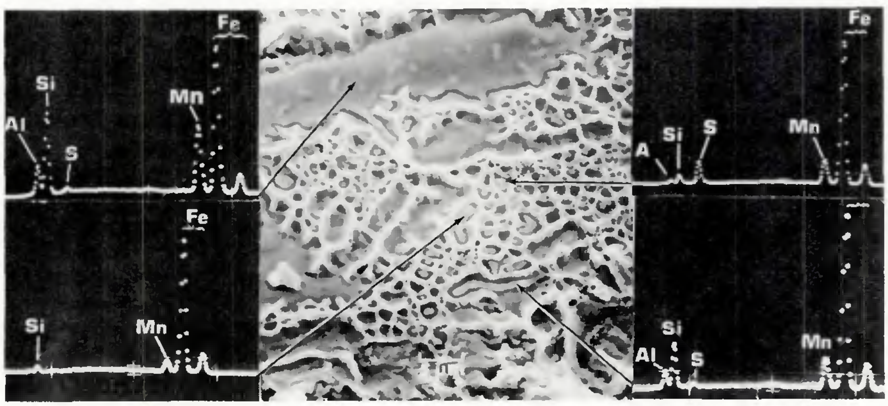

Fig. 16 — A large silicate surrounded by microvoids containing Fe rich oxides and oxysulfides in semikilled A-285 (M) steel. (X2000, reduced 42%)

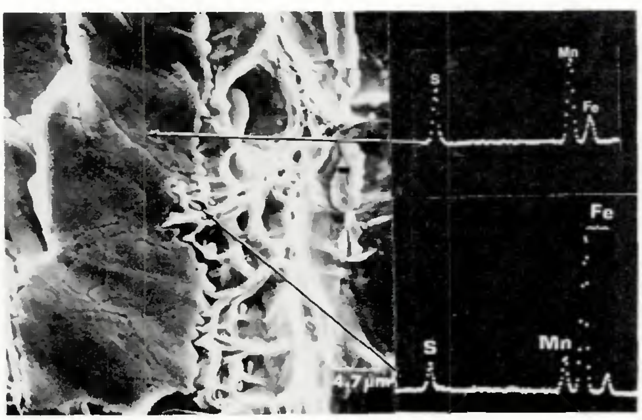

Fig. 17 — A large type III MnS beside a small type I oxysulfide in Al killed Mil 24113C (U). (X2150, reduced 40%)

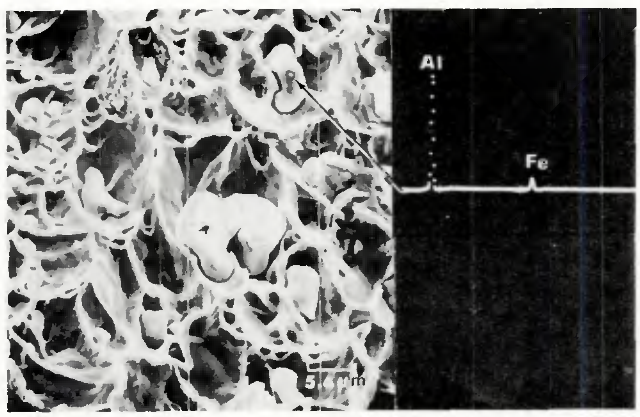

Fig. 18 — Voids containing alumina in Al killed Mil 24113C (U). (X1840, reduced 40%)

distribution of smaller inclusions is better than random distribution of larger inclusions.

While, in most cases, lamellar tearing initiated by void formation around inclusions, in some instances tearing was observed to occur by low energy mechanisms such as splitting along ferrite bands, liquation in reheated HAZ, and intergranular cracking. Thus, even a clean steel may readily initiate tearing according to the condition of the matrix and its susceptibility to HAZ embrittlement.

Void Growth

The extent of voids around inclusions was observed to vary among the various steels and tended to be greater among those displaying a high resistance to tearing (Fig. 25). Void extent is a measure of plastic work done and is influenced by the inter-inclusion spacing, matrix flow stress, nature of second-phase particles and the stress state. With an increase in the level of triaxiality and matrix flow strength, the plastic flow is inhibited in the matrix and tends to concentrate at the voids where the stresses are higher and the constraint is low. If the inclusions are closely spaced or if the intervening matrix is free of incoherent particles, then the voids continue to grow until they eventually link by necking. However, in the presence of small sulfides, oxides or other second phase particles in the matrix, void growth is limited and linkage occurs prematurely by a sheet of microvoids.

Void Linkage

The linking of elongated inclusion voids on the terrace was observed to occur by several modes such as necking, microvoid coalescence, "zig-zag" tearing, intergranular cracking, quasi-cleavage and cleavage (Figs. 26, 27). The amount of energy absorbed during tearing was dependent on which of these modes was dominant. Necking and microvoid coalescence were the commonly observed modes. In a few rare instances linkage occurred by a "zig-zag" mode of tearing. Such a mode has also been reported by other investigators (Refs. 64-66). Beachem (Ref. 64) has attributed it to a blend of shearing and tearing on alternating shear planes, causing the crack to follow a "zig-zag" course. This mechanism was not observed in the strongly banded plates.

In the quenched and tempered A533 Gr. B (D) steel, void linkage occurred by a combination of necking, microvoid coalesence and intergranular cracking. The intergranular mode of linkage was only observed in the HAZ, possibly due to some form of embrittlement. The quasi-cleavage mode of linkage was also confined to HAZ and the small cleavage-like facets suggest tearing through martensite laths (Fig. 27c).

The lack of a satisfactory correlation between the inclusion count and the tearing susceptibility, even among steels containing similar inclusion types, suggests that the smaller inclusions (oxides, sulfides, etc.), not represented in the Quantimet data, and other factors like crystallographic texture, banding, matrix embrittlement, etc. may exert significant influence on the tearing susceptibility. Thus, the greater susceptibility of semikilled A-285 (M), despite its lower inclusion count, as compared to semikilled A-36 (X), may be due to the presence of large amounts of smaller oxides and oxysulfides which limited the void growth

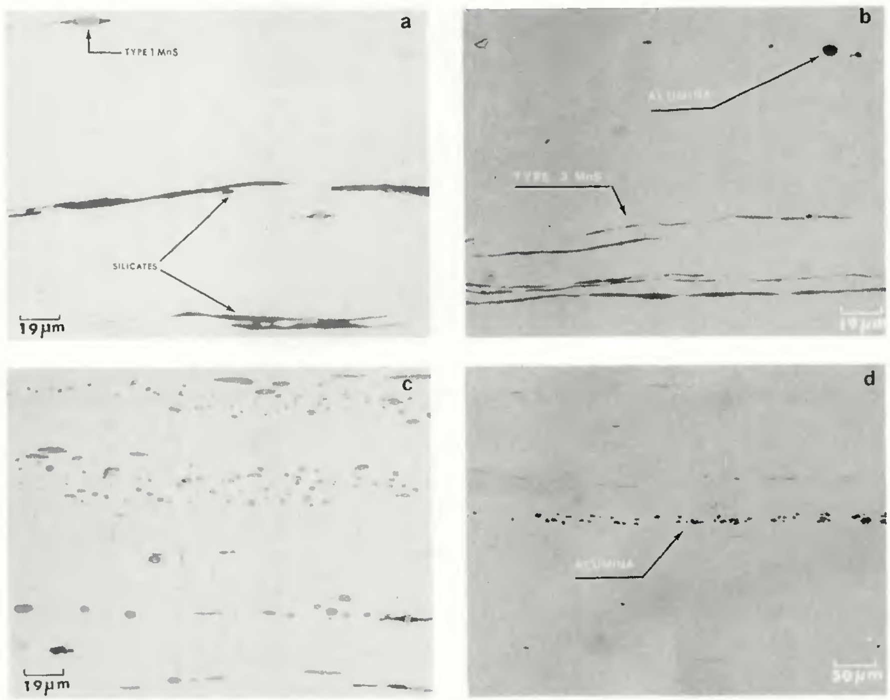

Fig. 19 — Inclusion distribution in some steels: (a) semikilled A-285 (M); (b) Al killed Mil 16113C (T); (c) Pb-sulfurized F. M. steel (N); (d) Al killed Mil 24113C (U). (Reduced 47%)

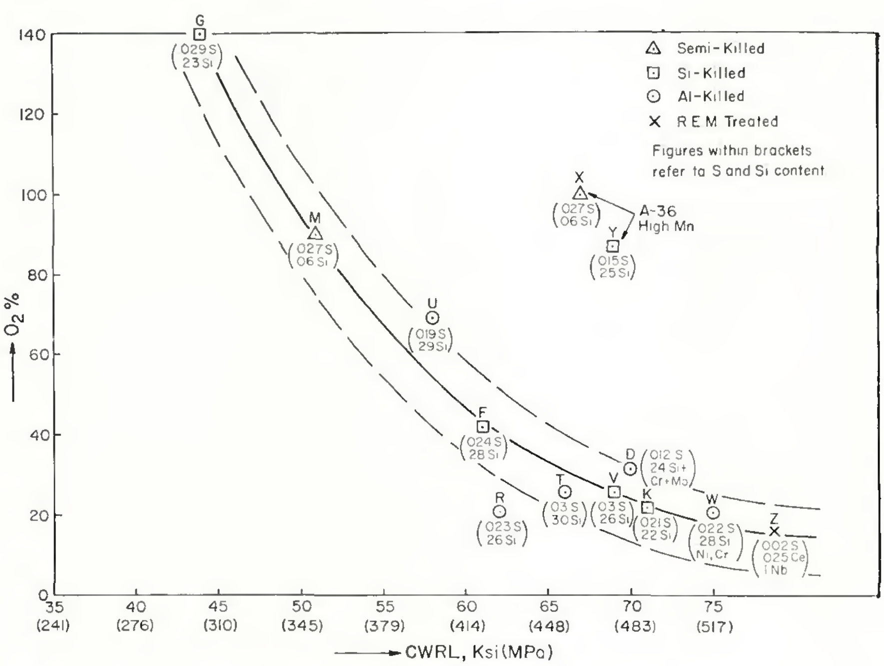

Fig. 20 — Oxygen vs susceptibility (CWRL)

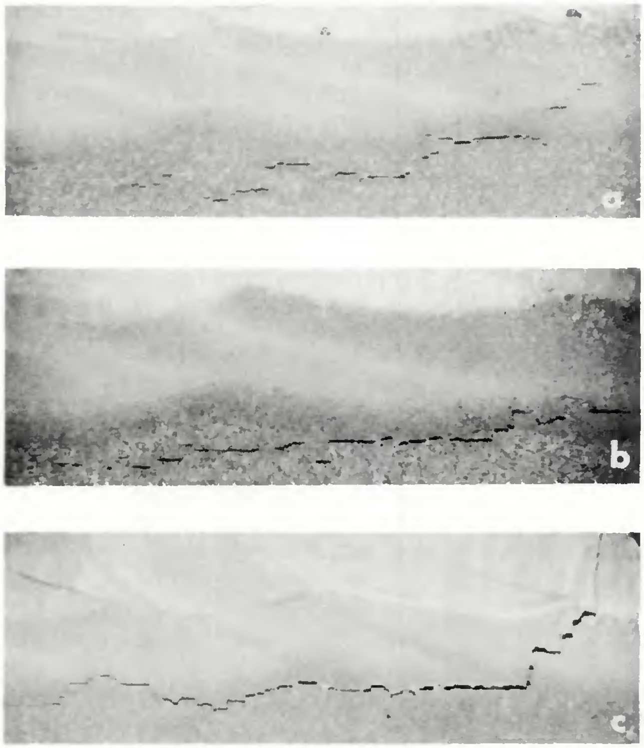

Fig. 21 — Progressive stages in lamellar tearing. (a) void formation; (b) terrace linkage; (c) shear linkage. A515-70 (F). (Reduced 22%)

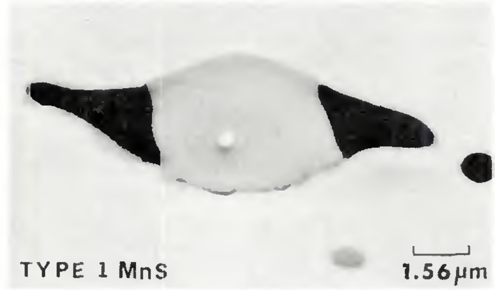

Fig. 22 — Decohered type I sulfide

Fig. 23 — Multiple internal fracture in a long sulfide. Note undamaged smaller sulfides

and caused premature linkage of inclusion voids whereas the A-36 (X) steel had relatively fewer oxides and oxysulfides, as is evident from the fractographs shown in Figs. 25a, b.

Thus, susceptibility to lamellar tearing is a function of the energy absorbed during each stage of tearing which, in turn, is controlled by a variety of metallurgical variables. While increasing the steel cleanliness is an obvious method of enhancing the tearing resistance, improvement may also be sought by:

1. Reducing the inclusion size and altering the shape by additions of innoculants, stirring of ladle, etc. so as to enhance nucleation.
2. Avoiding silicates and iron-rich oxides by adopting Al killed practice and adding sufficient amounts of Al to preserve an adequate cover until tapping.
3. Controlling the shape and size of sulfides through rare earth additions.
4. Proper choice of rolling conditions to reduce mechanical fibering, crystallographic texturing and banding.
5. Enhancing the matrix toughness of steel by reducing grain size, alloying, etc.

There are, thus, several metallurgical options available to produce steels with a high resistance to lamellar tearing and the choice of method is dictated by considerations of cost and criticality of application.

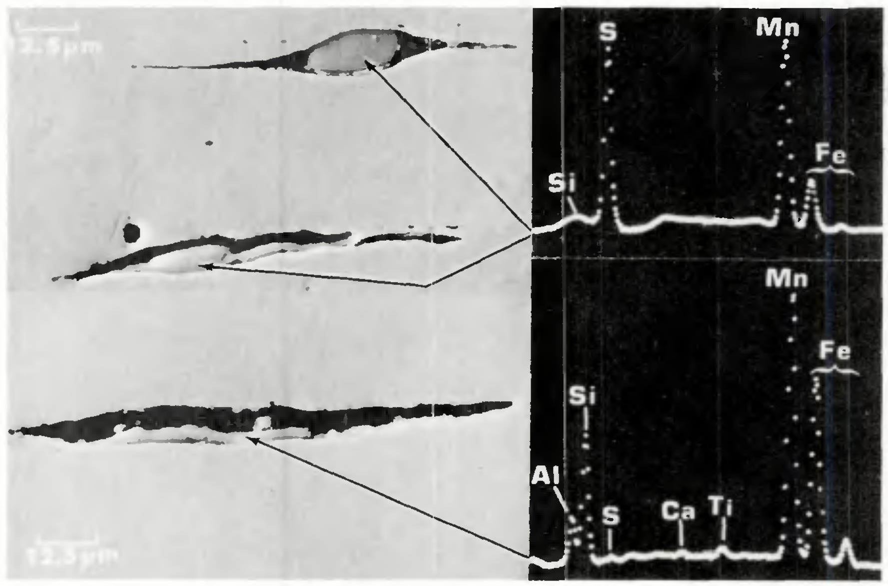

Fig. 24 — Decohered sulfides and a fractured silicate in ABS EH-33 (P) steel tested below CWRL. (X1600, reduced 22%)

Conclusions

1. Lamellar tearing is a complex phenomenon governed by a variety of metallurgical and mechanical variables and resistance to it cannot, therefore, be simply related to the steel grade, plate thickness, or the inclusion type.

2. Tearing susceptibility is mainly influenced by the material condition close to the plate surface and through-thickness properties ob-

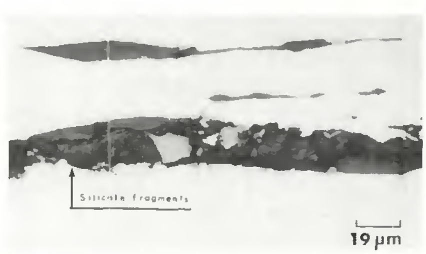

Fig. 25 — A fractured silicate beside undamaged smaller silicates in Si killed A-283 (B). (X533, reduced 40%)

tained at the center-thickness may be misleading.

3. While tearing is commonly associated with the elongated nonmetallic inclusions, initiation may also occur by splitting along sheets of fine inclusions, textured ferrite bands, and embrittled grain boundaries.

4. Susceptibility tends to increase with an increase in the oxygen content of the steel.

5. Larger inclusions tend to form voids earlier than the smaller ones.

6. It is unlikely that the inclusion count, using the prevailing techniques, would yield a satisfactory correlation with the lamellar tearing susceptibility, as these techniques disregard the smaller inclusions in the plate, which may exert significant influence on the tearing susceptibility, and the anisotropic effects induced by crystallographic texture, banding, and other microstructural factors.

Bibliography

1. "Lamellar Tearing of Steel Worries Designers," *Engineering News Record*, Sept. 21, 1972, p. 53.
2. "Lamellar Tearing Subject of Lawsuit," Ibid, March 20, 1975, pp. 39-40.
3. "AISC, Armco named third party defendants in lamellar tearing suit," Ibid, July 10, 1975, p. 16.
4. "Steel cracking causes design change, delays job," Ibid, January 29, 1976, p. 12.
5. Burdekin, F. M., "Lamellar Tearing in Bridge Girders — A Case History," *"Metal Construction and British Welding Journal*, Vol. 3, No. 5, May 1971, pp. 205-209.
6. Goodger, A. H., "Fissuring along the Flow Structure of a Plate Under Fillet Welds," *BSI News*, Sept. 1966, pp. 10-13.
7. Watanabe, Masaki, "The Pull-Cut Fracture in Rolled Steel Plate," *Symposium, Welding in Shipbuilding*, 1961, pp. 219-225, Institute of Welding, London.
8. Takeshi, Y., "Lamellar Tearing and Marine Structures," *Welding and Metal Fabrication*, Vol. 43, No. 10, December 1975, pp. 740-746.
9. Meyer, H. J., "Sub Surface Cracks in Plates at the Points of Application of Stresses Perpendicular to the Plate Surface," *Archiv Eisenhuttenw*, 35 (9), 1964, pp. 903-908. (Translated BWRA Bulletin (6), Oct. 1965).
10. Wormington, H., "Lamellar Tearing in Silicon-Killed Boiler Plate," *Welding and Metal Fabrication*, Vol. 30, No. 9, Sept. 1962, p. 370-373.
11. *Nucleonics Week*, World News, 8, April 17, 1969.
12. "Commentary on highly restrained welded connections," *Engineering Journal of AISC*, 1973, pp. 61-73.
13. Thornton, C. H., "Quality Control in Design and Supervision Can Eliminate Lamellar Tearing," *Engineering Journal of AISC*, Vol. 9, No. 6, 1973, pp. 112-116.
14. "Report on Enquiry into the Failure of Structural Members Stressed in the Direction of Plate Thickness," *Welding in the World*, Vol, 11, No. 7/8, 1973, pp. 44-47.

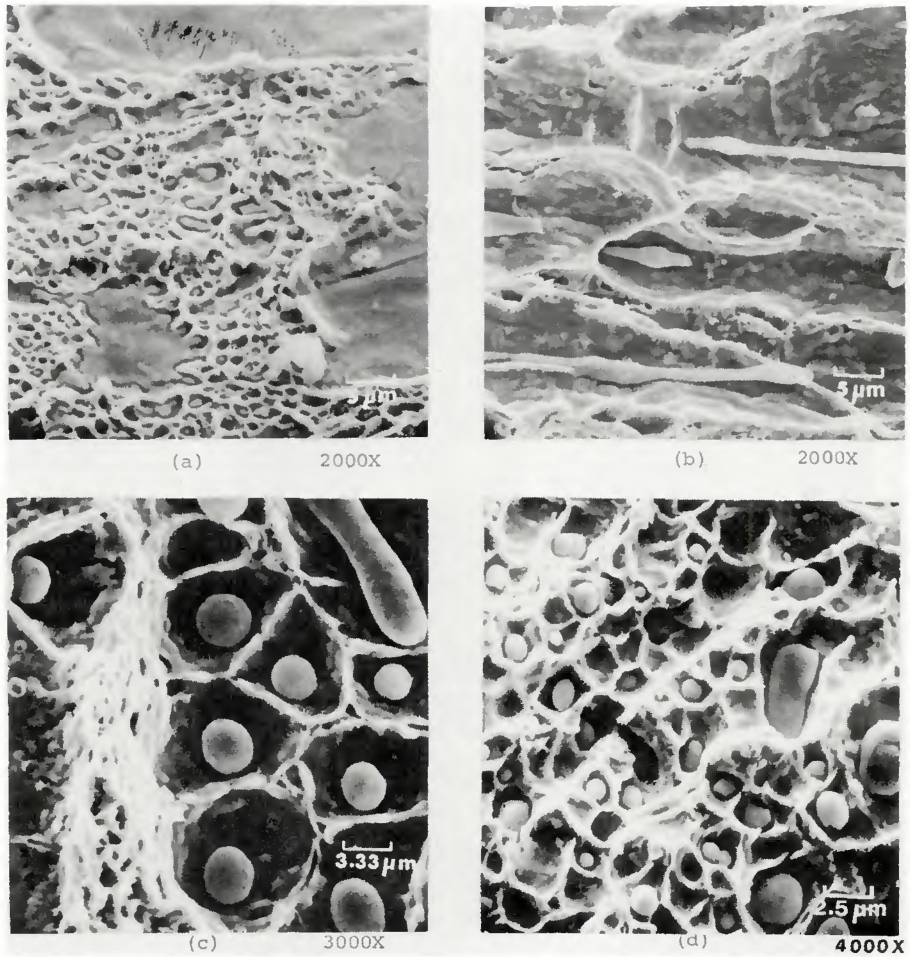

Fig. 26 — Extent of void growth around inclusions in various steels: (a) semikilled A-285 (M); (b) semikilled A-36 (X); (c) Al killed A533 Gr.B (D); (d) Pb-sulfurized F. M. steel (N). (Reduced 35%)

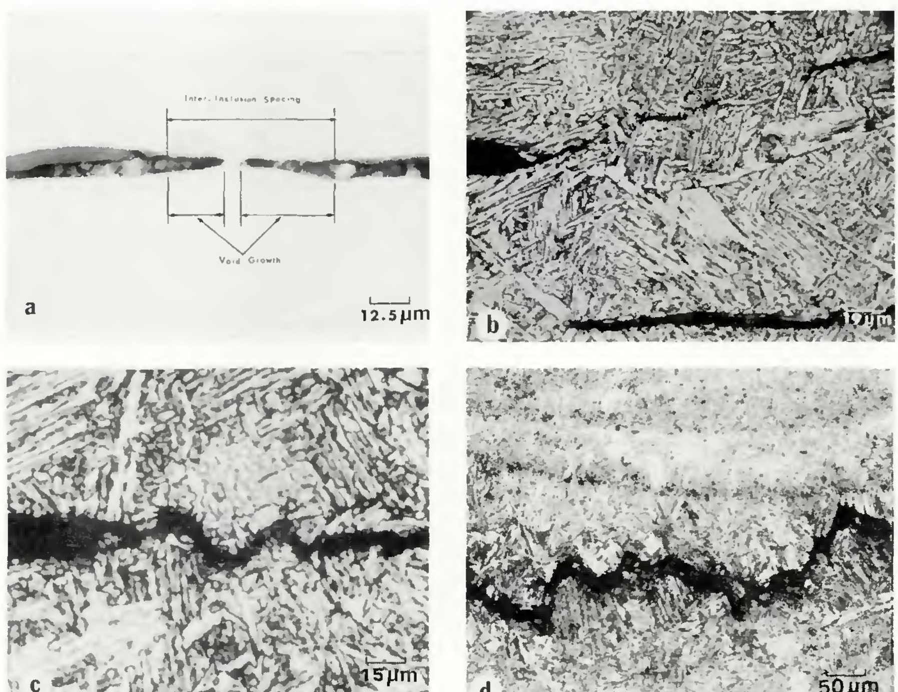

Fig. 27 — Types of terrace linkage: (a) necking; (b) microvoid sheets; (c) zig-zag tearing; (d) intergranular cracking

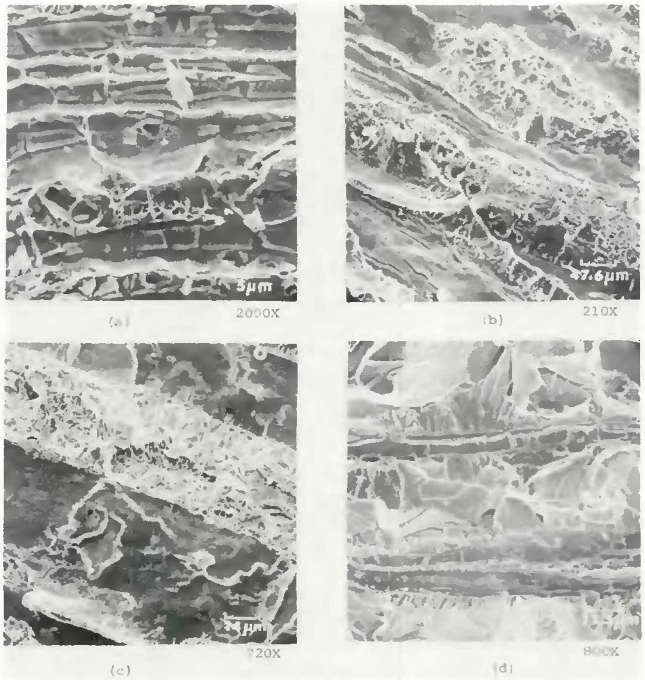

Fig. 28 — Types of void linkage: (a) necking; (b) microvoid coalescence; (c) quasi-cleavage; (d) cleavage. (Reduced 54%)

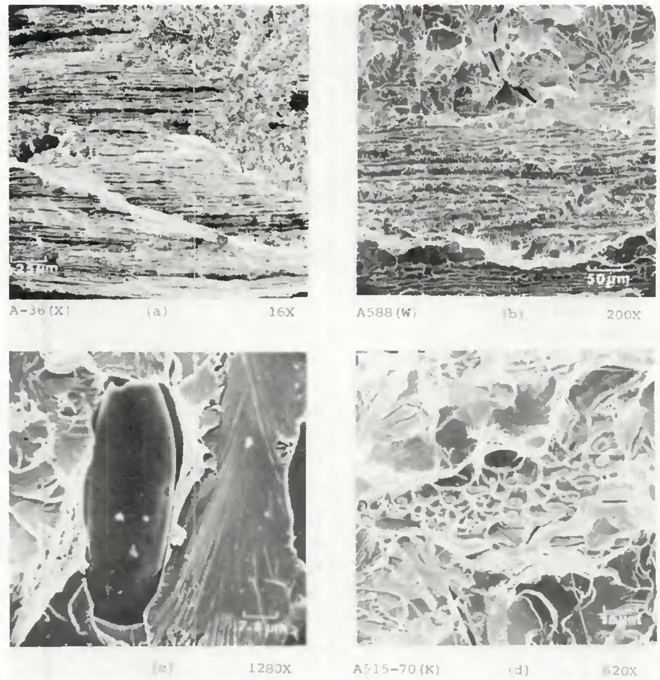

Fig. 29 — Lamellar tear and cleavage: (a) lamellar tear initiation and cleavage propagation; (b) transition zone from lamellar tear to cleavage; (c) sulfide within a void surrounded by cleavage facets; (d) cluster of dimples surrounded by cleavage. (Reduced 54%)

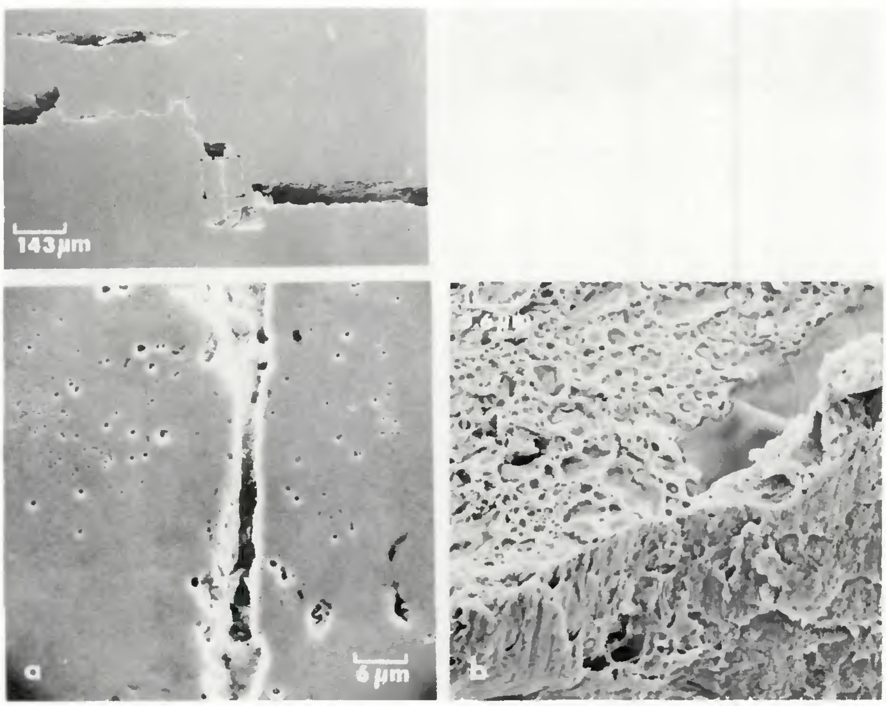

Fig. 30 — Shear linkage of terrace tears: (a) microvoids on either side of shear wall; (b) microvoids on the terrace as well as shear wall. (Reduced 32%)

15. "Discussion on Lamellar Tearing," *Metal Construction and British Welding Journal,* Vol. 1, No. 2, Feb. 1969, pp. 117-124.

16. Nagel, D. and Schonherr, W., "Strength and Deformation Properties of Structural Steels in the Direction of Thickness," *Metal Construction and British Welding Journal,* Vol. 1, No. 2, Feb. 1969, pp. 64-67.

17. Heuschkel J., "Lamellar Tearing," Private Communication with K. H. Koopman, Feb. 9, 1971.

18. Vrbensky, J., "Some Weldability Problems of Thin Mn-V-N Type Stress Plates from the Crackability Point of View," *Metal Construction and British Welding Journal,* Vol. 1, No. 2, Feb. 1969, pp. 44-49.

19. Lombardini, J., "Cracking as a Criteria for Weldability," *Metal Construction and BWJ,* Vol. 1, No. 2, Feb. 1969, pp. 40-43.

20. Nicholls, D. M., "Lamellar Tearing in Hot Rolled Steel," *British Welding Journal,* Vol. 15, No. 3, March 1968, pp. 103-112.

21. Amemya, Y., Satake, M., Kajimoto, K. and Ohba, K., "Effects of Welding Procedure and Steel Materials on Prevention of Lamellar Tearing," *International Institute of Welding,* Doc. No. IX-780-72, May 1972.

22. Oates, R. P. and Stout, R. D., "A Quantitative Weldability Test for Susceptibility to Lamellar Tearing," *Welding Journal,* Vol. 52, No. 11, Nov. 1973, pp. 481-491.

23. Nishio, Y., Yamamoto, Y., Kajimoto, K. and Hirozane, T., "On Lamellar Tearing in Multirun Fillet Welds," Technical Review, Vol. 9, No. 3, Oct. 1972, Mitsubishi Heavy Industries Ltd., Japan.

24. Bellen, A. Sparraft, M. J. and Vander Veen, J. H., "Some Steelmakers' Experience on Improving the Resistance of Steel Plate to Lamellar Tearing," *First International Symposium of the Japan Welding Society,* No. 8, 1971.

25. Elliott, D. N., "A Fractographical Examination of Lamellar Tearing in Multirun Fillet Welds," *Metal Construction and British Welding Journal,* Vol. 1, No. 2, Feb. 1969, pp. 50-57.

26. Farrar, J. C. M., Dolby, R. E. and Baker, R. G., "Lamellar Tearing in Welded Structural Steels," *Welding Journal,* 48 (7), July 1969, Research Suppl., pp. 274s-282s.

27. Jubb, J. E. M., Currick, L. and Hammond, J., "Some Variables in Lamellar Tearing," *Metal Construction and British Welding Journal,* Vol. 1, No. 2, Feb. 1969,

pp. 58-63.
28. Arita, Y. and Kajimoto, K., "The Study of Lamellar Tearing in Offshore Structure," *Fourth Annual Offshore Technology Conference in Houston, Texas,* May 1972.
29. Owen, W. S., Cohen, M. and Averbach, B. L., "The Influence of Ferrite Banding on the Impact Properties of Mild Steel," *Welding Journal,* 37 (8), Aug. 1958, Research Suppl., pp. 368s-374s.
30. Farrar, J. C. M. and Dolby, R. E., "An Investigation into Lamellar Tearing, *Metal Construction and British Welding Journal,* Vol. 1, No. 2, Feb. 1969, pp. 32-34.
31. Araki, M., et al., "Cracking in Multirun Fillet Welds," Nippon Kokan Technical Report-overseas, June 1974, pp. 25-35.
32. Nicholls, D. M., Wilson, D. M. and Jubb, J. E. M., "Correspondence on Lamellar Tearing," *British Welding Journal,* Vol. 13, No. 5, May 1966, pp. 326.
33. Golikov, I. N., "Certain peculiarities in the formation of oxide-inclusions revealed by complex analysis," in 'Production and Application of Clean Steels,' ISI, Sp. report, ISI London, 1970, pp. 35-41.
34. Keissling, R., "The Influence of Non-Metallic Inclusions on the Properties of Steel," *J. Metals,* Vol. 22, No. 10, Oct. 1969, pp. 48-54.
35. Little, J. H. and Henderson, W. J. M., "Effect of Sulfide Inclusions on the Anisotropy of Ductile Charpy Shelf Energy," in 'Effect of Second Phase Particles on the Mechanical Properties of Steel,' ISI, Sp. Report, ISI, London, 1971, pp. 171-181.
36. Baker T. J. and Charles, J. A., "Morphology of Manganese Sulfide in Steel," *JISI,* September 1972, pp. 702-6.
37. Baker, T. J. and Charles, J. A., "Deformation of Manganese Sulfide Inclusions in Steel," Ibid, pp. 680-690.
38. Santen, S. and Ohman, B., "Techniques for obtaining extremely low contents of sulfur in steel under oxidizing and reducing conditions," Clean Steel, v. 1, Report of the Royal Swedish Academy of Engineering Sciences, 169:1, 1971, pp. 7-19.
39. Pickering, F. B., "Effect of Processing Parameters on the Origin of Nonmetallic Inclusions, in "Effect of Second Phase . . .," ISI, Sp. Report, ISI, London, 1970, pp. 75-91.
40. Keissling, R. and Nordberg, H., "Influence of Inclusions on the Mechanical Properties of Steel" in 'Production and Application of Clean Steels' ISI, Sp. Report, ISI, London, 1970, pp. 179-185.
41. Brooksbank, D. and Andrews, K. W., "Stress Fields Around Inclusions and Their Relation to Mechanical Properties," Ibid, pp. 186-198.
42. Allmand, T. R. and Blank, J. R., "An Evaluation of the Quantimet for Assessing Non-Metallic Inclusions and Other Microscopical Features in Metals and Alloys," in 'Automatic Cleanness Assessment of Steel," ISI, Sp. Report, No. 112, ISI, London, 1968, pp. 47-60.
43. Melford, "Design and Use of Automatic Instruments for Cleanness Assessment," Ibid., pp. 14-23.
44. Charpentier, P. L. et al., "Black-line surface defects in aluminum-killed steels," *Metals Technology,* Vol. 2, part 2, February 1975, pp. 52-61.
45. Cairns, R. L. and Charles, J. A., "Banding in carbon and low-alloy steel — a brief review," *Iron and Steel,* Vol. 39, November 1966, pp. 511-515.
46. Jatczak, E. F., Girardi, D. J. and Rowland, E. S., "On Banding in Steel," *Trans. A.S.M.,* Vol. 48, 1956, pp. 279-305.
47. Grange, R. A., "Effect of Microstructural Banding in Steel," *Metallurgical Transactions,* Vol. 2, February 1971, pp. 417-426.
48. Coleman, T., Dulien, D. and Gouch, A., "The structure and properties of controlled processed high strength ferrite-pearlite steels," in *Microstructure and Design of Alloys,* Vol. 1, 1974, London, The Metals Society, pp. 70-74.
49. Hero, H., Evensen, J. and Embury, J. D., "The occurrence of delamination in a controlled rolled HSLA steel," *Canadian Met. Quarterly,* Vol. 14, No. 2, 1975, pp. 117-122.
50. Yen, C. M. and Stickels, C. A., "Lamellate fracture in 5150 steel processed by modified ausforming," *Metallurgical Transactions,* Vol. 1, Nov. 1970, pp. 3037-3047.
51. Stoloff, N. S., "Effects of alloying on fracture characteristics," *Fracture,* Vol. VI, Edited by Liebowitz, H., Academic Press, N.Y. 1969, pp. 1-81.
52. Boniszewski, T. and Moreton, Mrs. J., "Effect of microvoids and manganese sulfide inclusions in steel on hydrogen evolution and embrittlement," *British Welding Journal,* Vol. 14, No. 6, June 1967, pp. 321-336.
53. Moreton, Mrs. J., Coe, F. R. and Boniszewski, T., "Hydrogen movement in weld metals," *Metal Construction and British Welding Journal,* Vol. 3, No. 5, May 1971, pp. 185-187.
54. Hewitt, J. and Murray, J. D., "Effect of sulfur on the production and fabrication of C-Mn steel forgings," Ibid, Vol. 1, No. 2, Feb. 1969, pp. 24-31.
55. Smith, N. and Bagnall, B. I., "The influence of sulfur on HAZ cracking of C-Mn steel welds," Ibid, pp. 17-23.
56. "Discussion of hydrogen Induced cold cracking," Ibid. pp. 109-116.
57. Argon, A. S. and Im, J., "Separation of Second Phase Particles in Spherodized 1045 Steel, Cu-0.6% Cr Alloy and Maraging Steel in Plastic Straining," *Metallurgical Transactions A,* Vol. 6A, April 1976, pp. 839-851.
58. Gangulee, A. and Gurland, J., "On the Fracture of Silicon Particles in Aluminum-Silicon Alloys," TMS-AIME, Vol. 239, Feb. 1967, pp. 269-272.
59. Gurland, J., "Observations on the Fracture of Cementite Particles in a Spherodized 1.05% C Steel Deformed at Room Temperature," *Acta Met.,* Vol. 20, May 1972, pp. 735-74.
60. Cox, T. B. and Low, J. R., "An Investigation of the Plastic Fracture of AISI 4340 and 18-Nickel-200 Grade Maraging Steels," *Metallurgical Transactions,* Vol. 5, June 1974, pp. 1457-1470.
61. Van Stone, R. H. and Psioda, J. A., "Discussion of Metallurgical Factors Affecting Fracture Toughness of Aluminum Alloys," *Metallurgical Transactions A,* Vol. 6A, April 1975, pp. 668-670.
62. Argon, A. S., Im, J. and Safoglu, R., "Cavity Formation from Inclusions in Ductile Fracture," *Metallurgical Transactions A,* Vol. 6A, April 1975, pp. 825-836.
63. Schulz, B. J. and McMahon, C. J., Jr., "Alloy Effects in Temper Embrittlement" in "Temper Embrittlement of Alloy Steels," ASTM STP 499, ASTM, 1972, pp. 104-135.
64. Beachem, C. D. and Yoder, G. R., "Elastic-Plastic Fracture by Homogeneous Microvoid Coalescence Tearing Along Alternating Shear Planes," *Met. Trans.,* Vol. 4, April 1973, pp. 1145-1153.
65. Chipperfield, C. G. and Knott, J. F., "Microstructure and Toughness of Structural Steels," *Metals Technology,* Vol. 2, Feb. 1975, pp. 45-51.
66. Knott, J. F., "Mechanics and Mechanisms of Large Scale Brittle Fracture in Structural Metals," *Materials Science and Engineering,* Vol 7, Jan. 1971, pp. 1-36.